Root-TRAPR: a modular plant growth device to visualize root development and monitor growth parameters, as applied to an elicitor response of Cannabis sativa

Pipob Suwanchaikasem (psuwanchaika@student.unimelb.edu.au)
University of Melbourne School of BioSciences https://orcid.org/0000-0001-7991-6414
Robert Walker
University of Melbourne School of BioSciences
Alexander Idnurm
University of Melbourne School of BioSciences
Jamie Selby-Pham
University of Melbourne School of BioSciences
Berin A. Boughton
Murdoch University

Methodology

Keywords: 3D printing, chitinase, chitosan, EcoFAB, exudate, hydroponic, industrial hemp, peroxidase, plant defense, phytohormone

Posted Date: August 2nd, 2021

DOI: https://doi.org/10.21203/rs.3.rs-764290/v1

Version of Record: A version of this preprint was published at Plant Methods on April 9th, 2022. See the published version at https://doi.org/10.1186/s13007-022-00875-1.

Abstract

Background

Plant growth devices, for example rhizoponics, rhizoboxes, and ecosystem fabrication (EcoFAB) have been developed to facilitate studies of plant root morphology and plant-microbe interactions in controlled laboratory settings. However, several of these designs are suitable only for studying small model plants such as *Arabidopsis thaliana* and *Brachypodium distachyon*, and therefore require modification to be extended to larger plant species like crop plants. In addition, specific tools and technical skills required for fabricating these devices may not be available to researchers. Hence, this study aimed to establish an alternative protocol to generate a larger, modular and reusable plant growth device based on differently available resources.

Results

Root-TRAPR (Root-Transparent, Reusable, Affordable three-dimensional Printed Rhizo-hydroponic) system was successfully developed. It consists of two main parts, an internal root growth chamber and external structural frame. The internal root growth chamber is comprised of a polydimethylsiloxane (PDMS) gasket, microscope slide and acrylic sheet while the external frame is printed from a three-dimensional (3D) printer and secured with nylon screws. To test the efficiency and applicability of the system, industrial hemp (*Cannabis sativa*) was grown with or without exposure to chitosan, a well-known plant elicitor used for stimulating plant defense. Plant root morphology was clearly detected in the system and plant tissues were easily collected and processed to examine plant biological responses. Upon chitosan treatment, chitinase and peroxidase activities increased in root tissues (1.7- and 2.3-fold, respectively) and exudates (7.2- and 21.6-fold, respectively). Phytohormones related to plant growth and defense response were higher in root tissues as compared to the shoots. Additionally, within two weeks of observation, hemp plants exhibited dwarf growth in Root-TRAPR system, easing plant handling and allowing increased replication under limited growing space.

Conclusion

The Root-TRAPR system facilitates exploration of root morphology and root exudate of *C. sativa* under controlled conditions and at a smaller scale. The device is easy to fabricate and applicable for investigating plant responses toward elicitor challenge. This fabrication protocol is modifiable to suit other plants and can be adapted to study plant physiology in other biological contexts, such as plant responses against biotic and abiotic stresses.

Background

In nature, plant roots develop underground and in sophisticated associations with microorganisms, making it difficult to observe root structure and conduct research on root activities [1]. Several platforms, for example rhizotrons [2], rhizoponics [3] and rhizoboxes [4] have been developed to facilitate plant root morphological studies in controlled laboratory settings. Technologies like Plant-in-Chip [5], RootChip [6], tracking roots interaction system (TRIS) [7] and ecosystem fabrication (EcoFAB) [8] have been further modified to increase the accessibility of plant-microbe interaction analysis. These systems are custom-made, requiring specialized techniques, tools and settings for manufacturing and implementing, therefore modification of the designs may be necessary upon the availability of different resources and intended research application.

One of the most recent examples, EcoFAB (https://eco-fab.org/) is an inexpensive and easy-to-fabricate device, built based on three-dimensional (3D) printing technology [9, 10]. The original iteration is constructed using a microscope glass slide bonded via a plasma cleaner to a custom-built polydimethylsiloxane (PDMS) growth chamber. The PDMS section is cast in a plastic mold, printed from a 3D printer. Optionally, an attachment between the glass slide and PDMS layer can be reversibly bound using a 3D printed plastic or a machined metal clamp. The EcoFAB model has a number of benefits. It enables readily accessible observation of root morphology and microbial localization using microscopes and other non-destructive imaging tools. Root biochemical and exudate composition can be collected and analyzed under standardized procedures. The model can use different growth substrates such as soil, sand and liquid [9]. Reproducibility of the EcoFAB device has been verified across multiple laboratories in diverse growth environments [11]. The versatility of the EcoFAB system permits robust studies on model plants such as *Arabidopsis thaliana*, *Brachypodium distachyon* and *Panicum virgatum*. Although it is appropriate for the use on these model plants, a larger device is required to address research questions in a broader array of plant species like staple and industrial crops which are generally longer lived and grow to larger sizes as compared to the model plants. Moreover, technical support including 3D printers, plastic materials and accompanying tools may vary across different workplaces. Hence, manufacturing processes are dependent upon availability of the relevant machineries and supplies.

Industrial hemp (*Cannabis sativa*) is an emerging crop within the agricultural industry worldwide [12]. Its global market is projected to increase from $3.5 billion in 2019 to $18.8 billion in 2025 with a compound annual growth rate of 32.17% [13]. Hemp seed contains low tetrahydrocannabinol (THC) content but high amount of protein and good proportion of healthy unsaturated fatty acids [14, 15], creating the demand in food and beverage industries. Hemp seed oil is used as a nutritional supplement and is added into skincare and medicinal products [12, 16]. Hemp fiber is a perfect source for the textile industry owing to its robustness and high absorbent capacity [17] and hemp hurd has been increasingly processed into hempcrete to replace traditional concrete in construction and building [18].

Despite its benefits, fundamental research to inform and establish daily agronomical practice has been lacking and inconclusive for the growers, who have been unable to transform scientific data into field applications [19]. For example, *C. sativa* is infected by a number of pathogenic fungi such as *Botrytis*

cinerea causing grey mold, *Fusarium* and *Pythium* species causing root rot, *Macrophomina phaseolina* causing charcoal rot, *Sclerotinia sclerotiorum* causing stem canker and *Golovinomyces cichoracearum* causing powdery mildew [20–22]. These infections suppress plant growth, reduce yield and product quality in both outdoor fields and greenhouse settings [21]. However, the pathology underlying the different infections is currently poorly understood and disease management programs have not been fully established [22]. The growers may apply inorganic agents, for example potassium bicarbonate, hydrogen peroxide, boric acid, orthosilicic acid or synthetic fungicides such as fluopyram to moderate or eradicate fungal pathogens [23]. To avoid the use of chemicals, natural products such as seaweed extract, plant growth-promoting bacteria, humic substances and chitin/chitosan derivatives have been used to increase product yield and promote plant defense to combat pests and diseases in other crops [24, 25]. They can be mixed into the soil or diluted and sprayed on aboveground plant tissues [26, 27]. Nonetheless, the benefits of any approach have not yet been comprehensively examined in *C. sativa* plants. Verifying their stimulating effects will benefit both industrial hemp and medicinal cannabis (high-THC cultivars) industries to tackle fungal disease problems in the field.

As principally inspired by the EcoFAB model, we developed a new device called Root-Transparent, Reusable, Affordable 3D Printed Rhizo-hydroponic or Root-TRAPR system. The device was enlarged and strengthened to cope with industrial hemp growth. To demonstrate the usability and effectiveness of the system, an elicitor challenge assay using colloidal chitosan was developed, and its effect was examined on plant defense by monitoring plant root development and analysis of biological responses by measuring specific enzymatic activities and phytohormone levels. Root-TRAPR system could be a convenient testing platform for verifying stimulating effects of plant elicitors on *C. sativa* plants to further the goals of sustaining and promoting the expanding cannabis industry.

Results

Generation of Root-TRAPR system

Through a process of iterative design, the Root-TRAPR system was created based on available resources at the University of Melbourne, Australia. The model was inspired by a range of plant growth devices, including the recent EcoFAB model developed at Lawrence Berkeley National Laboratory, US [9]. We retain certain elements of the original EcoFAB design including a glass microscope slide base with PDMS layer. Differently, our chamber is enclosed by an acrylic sheet, sealed using a compression seal which is supported by a 3D-printed external structural frame. An exploded-view diagram displaying the components of Root-TRAPR system and the assembly is shown in Fig. 1. Representatives of the system and all components are featured in Fig. 2 and the details of each part are described in Table 1.

Root-TRAPR system is comprised of two major components – an internal root growth chamber (Fig. 2c) and an external structural frame (Fig. 2d). The internal root growth chamber has a transparent viewing configuration from either top or bottom sides by use of a clear acrylic sheet and microscope slide, respectively to facilitate plant root structure observation. A square PDMS gasket with an oval void in the

center is pre-cast in a 3D-printed plastic mold (Fig. 2e), which enables fine tuning of the void volume by increasing/decreasing the oval width or gasket thickness. The elastic gasket is inserted between the acrylic sheet and microscope slide to create a root growth chamber. The acrylic sheet is pre-drilled with upper and lower holes for inserting the plant seed and exchanging plant growing media, respectively.

The three internal layers comprised of acrylic sheet, PDMS gasket and microscope slide are secured and compressed using top and bottom external frames printed from a fused deposition modeling (FDM) 3D printer using an inexpensive polylactic acid (PLA) plastic material. The frame is furnished with 8 sets of nylon bolts and hexagon nuts (Fig. 2f) to tightly fasten and compress the whole model together. A rubber bung (Fig. 2g) is plugged into the lower smaller hole of the acrylic sheet to stop leakage. During growth experiments, the stand (Fig. 2h) and window shutter (Fig. 2i) can be additionally put in place to tilt the model at a 25° angle to promote gravitropism and to prevent direct light onto the plant roots, respectively. The assembled Root-TRAPR device is not damaged by absolute ethanol, therefore the model can be submerged in the solvent for decontamination and sterilization prior to use.

Approximate cost of Root-TRAPR system is detailed in Table 1. All 3D-printed objects are subjected to a subsidized $0.15 AUD per 1 g material according to the standard printing price for staff and students of the University of Melbourne [28]. Total cost is approximately $64.0 AUD per unit but could vary based on differing plastic materials, printing resolution, machinery techniques or bulk supplies used.

Table 1
Details and cost of each component in Root-TRAPR system.

No.	Component	Material	Size	Approximate Cost (AUD) per unit	Supplier
1	PDMS mold	PLA	External: 138×94 mm Internal: 130×86 mm	$9.0	Printed from a 3D printer
2	PDMS layer - Void oval chamber	PDMS (Sylgard 184)	130×86 mm; 3 mm - 100×64 mm	$6.5	Cast in the PDMS mold
3	Microscope slide	Glass	128×85 mm; 1 mm	$2.5	ProSciTech, Australia
4	Acrylic sheet - Small hole - Large hole	Transparent acrylic plastic	128×85 mm; 1.5 mm - 8 mm in diameter - 9 mm in diameter	$2.0	Warlond Plastics, Australia
5	Rubber bung	rubber	8×13 mm; 19 mm	$0.5	Pacific Laboratory Products, Australia
6	Top frame	PLA	External: 162×119 mm; 3.5 mm Internal (oval): 130×90 mm; 4 mm	$15.0	Printed from a 3D printer
7	Bottom frame	PLA	External: 162×119 mm; 9 mm Internal: 132×88 mm; 6.5 mm	$19.0	Printed from a 3D printer
8	Cheese head bolts (8 pieces)	Nylon	5×40 mm	$2.5	Keables, Australia
9	Hexagon nuts (8 pieces)	Nylon	5 mm	$1.0	Keables, Australia
10	Window shutter	PLA	106×70 mm; 2 mm	$4.0	Printed from a 3D printer

No.	Component	Material	Size	Approximate Cost (AUD) per unit	Supplier
11	Stand	PLA	72×50 mm; 3 mm	$2.0	Printed from a 3D printer
			Total	$64.0	

Industrial hemp growth in Root-TRAPR system

Plant growth experiments were carried out using three biological replicates under two different conditions – control and chitosan treatment. After germination in petri dishes, industrial hemp seedlings were transferred to Root-TRAPR systems and maintained for 14 days in a controlled environment with Hoagland nutrient solution (Additional file 1). After 7-days of growth, nutrient solutions were exchanged by which control plants was treated with standard Hoagland solution and chitosan treatment was performed by substituting plain Hoagland solution with the solution containing 1% w/v colloidal chitosan. Plant growth was monitored with root structure recorded every 2–3 days using a modified scanner connected with WinRHIZO software. Upon harvest on day 14, plant root and shoot tissues along with root exudate were collected and subsequently processed for enzymatic assays, phytohormone quantifications and gene detections.

Root morphology was clearly observed using images captured by a well-calibrated optical light scanner and analyzed by WinRHIZO software throughout the study (Fig. 3). Root growth was monitored through three different parameters – root length, root surface area and average root diameter. Under control conditions, plants constantly expanded their roots throughout 14 days of observation, ending at 55.27 ± 5.06 cm and 12.33 ± 1.35 cm^2 in length and surface area, respectively (Fig. 4a-d). The expansion rate was slow during the first week (from 5.47 to 16.49 cm in length and 1.17 to 3.32 cm^2 in surface area) but increased during the second week (from 16.49 to 55.27 cm in length and 3.32 to 12.33 cm^2 in area). Despite enlarging in root length and surface area, the average root diameter did not change during the monitoring period (from 0.72 to 0.71 mm; Fig. 4e-f). This indicates that plants expanded existing roots to a larger size and at the same time generated new lateral roots. Young secondary and tertiary branch roots, ranging between 0.2–0.5 mm in diameter offset the larger primary and pre-existing branch roots (Fig. 3), therefore average root diameter of the control plants remained constant.

In the chitosan-treated group, plant roots were well developed before chitosan was introduced on day 7, cumulative at 10.98 ± 3.65 cm in total root length and 2.28 ± 0.63 cm^2 in root surface area, which were not significantly different from the controls (Fig. 4a-d). However, after the treatment plants displayed significantly reduced root expansion, finishing at 12.79 cm ± 3.89 in length and 2.91 ± 0.80 cm^2 in surface area, which were significantly smaller than those of control plants (p-value = 0.003 and 0.004, respectively). The average root diameter was slightly increased after the treatment, expanding from 0.69 ± 0.05 mm (day 7) to 0.74 ± 0.02 mm (day 14) but was not statistically significant and did not differ from the controls (Fig. 4e-f). As observed from the root morphology (Fig. 3), chitosan-treated plants generated

remarkably fewer new branch roots as compared to the controls. This could reflect the slight increase of root diameter of chitosan-treated plants.

The reduction of root expansion by chitosan exposure was potentially due to the viscous properties of 1% w/v colloidal chitosan suspension. The solution turned into a gel-like suspension after chitosan was added into a Hoagland base liquid. Based on experimental measurement, 1% w/v chitosan is 13.72 times more viscous than water [29]. This physical gelatinous texture of the chitosan suspension may be one of the factors obstructing root development. In addition, its osmolality is 72 mOsm/kg in water [29], and when dissolved in Hoagland solution it is approximately 94 mOsm/kg. These two values indicate that the suspension should have minimal impact on plant nutrient uptake and tonicity in plant cells, where intracellular values typically range between 300–700 mOsm/kg [30].

To assess the health of the plants grown in Root-TRAPR system, hydrogen peroxide (H_2O_2) content was measured in root and shoot tissues and compared to the plants grown in a mini hydroponic-like system (Additional file 2). Levels of H_2O_2 in both shoots and roots were comparable between control and chitosan-treated plants (Fig. 5). In control, it was 9.61 ± 2.40 and 0.61 ± 0.08 µmol/g fresh weight (FW) in shoots and roots, respectively. This was 9.68 ± 1.48 µmol/g FW in shoots and 0.52 ± 0.15 µmol/g FW in roots of chitosan-treated plants. They were slightly higher than those of the plants grown in hydroponic device (6.61 ± 0.62 and 0.31 ± 0.11 µmol/g FW in shoots and roots, respectively) but statistical analysis using one-way analysis of variance (ANOVA) showed no significant differences for shoot and root tissues with p-value of 0.60 and 0.64, respectively. This suggests that plants were not stressed when grown in Root-TRAPR system and chitosan did not introduce stress to the plants. Moreover, H_2O_2 content measured from shoot tissues fell within the range detected from the leaves of experimental control plants in other studies. It was 5–10 µmol/g FW in reed [31] and nearly 6 µmol/g FW in marigold [32]. The level was slightly higher than normal range (0.5-4 µmol/g FW) measured from various plants including soybean, ground-ivy, bur oak, common blue violet and red mangrove under natural condition. However, environmental and experimental factors should be taken into account [33].

Furthermore, hemp plants grown in Root-TRAPR systems developed into a smaller size as compared to the plants typically potted in soil (Additional file 3). After two weeks of propagation, potted plants and control plants in Root-TRAPR systems produced the same number of leaves (6–10 leaves) and leaf nodes (2–3 nodes). However, plants in Root-TRAPR system had extremely shorter height and smaller leaves. In turn, the dwarf size of the plant in Root-TRAPR system would benefit cannabis plant research. It scales down plant size which could reduce maintenance costs and save plant growing space, usually limited in controlled laboratory conditions. Nonetheless, research findings would still be transferable as the plants grown in Root-TRAPR system showed natural and healthy development at vegetative phase.

Analytical measurements

After completing plant growth observation, shoot and root tissues along with root exudate were harvested and biochemical analyses including enzymatic assays, phytohormone quantification and DNA gene

determination were subsequently carried out to demonstrate the utility of Root-TRAPR system for plant sample collection and the suitability for subsequent assays to examine plant responses. Herein, the results generated from combining analytical techniques were integrated to primarily assess the effect of chitosan treatment on *C. sativa* plant.

Enzymatic activities

Peroxidase and chitinase are well-known plant pathogenesis-related proteins which play an important role in counteracting fungal attack [34, 35]. In this study, peroxidase and chitinase activities were measured in plant samples of shoot, root tissues and root exudate. Tissue samples (shoot and root) were harvested on the last day of experiment (day 14), whereas root exudate was collected twice on day 7 (pre-chitosan treatment) and day 14 (post-chitosan treatment). It was hypothesized that if chitosan treatment could stimulate the production of plant defense enzymes, a corresponding increase of peroxidase and chitinase activities would be observed. In parallel, protein concentrations of the samples were determined using Bradford assay and later used for data normalization.

When normalized to an equivalent amount of tissue fresh weight, total protein pools extracted from shoot tissues were 5–8 times higher than those extracted from the roots (Table 2). However, shoot tissues expressed lower activities of peroxidase and chitinase enzymes as compared to those in root tissues. In control plants, shoot expressed peroxidase activity at 0.51 ± 0.12 ΔOD/min·mg protein which was approximately 25-fold lower than that detected in root at 13.17 ± 0.80 ΔOD/min·mg protein. In chitosan-treated plants, peroxidase activity in shoot (0.66 ± 0.11 ΔOD/min·mg protein) was not different from that in control plants but was doubly increased in root tissues (30.80 ± 8.06 ΔOD/min·mg protein) with marginally significant difference (p-value = 0.09) as relative to control.

A similar tendency was observed for chitinase activity. In shoot tissues, it was equivalent at 0.21 mmol *N*-acetylglucosamine (GlcNAc) released per g protein between control and chitosan groups. The activity was slightly higher in root tissues of chitosan-treated plants (0.85 ± 0.11 mmol GlcNAc released per g protein) as compared to the control (0.51 ± 0.20 mmol GlcNAc released per g protein) but not significant (p-value = 0.22).

In root exudates (Table 3), measured protein concentrations were correlated with the volume of plant roots – the larger of the roots, the higher amount of proteins found in the exudate. In control plants, protein content was measured at 53.80 ± 11.91 µg/ml on day 7 which was approximately tripled by day 14 (146.20 ± 15.52 µg/ml). Proteins in root exudate of chitosan-treated plants were 81.07 ± 16.99 µg/ml on day 7 and only increased to 104.87 ± 11.14 µg/ml by day 14. As observed from root morphology (Fig. 3), chitosan-treated plants barely expanded their root after the treatment (10.98 cm on day 7 and 12.79 cm on day 14 in total root length) which would likely result in decreased protein secreted in its exudate on day 14. Peroxidase activity of the pre-treatment exudate was not different between control (0.04 ± 0.01 ΔOD/min·mg protein) and chitosan groups (0.13 ± 0.04 ΔOD/min·mg protein). However, the activity increased 50-fold to 6.48 ± 2.17 ΔOD/min·mg protein in post-treatment exudate of chitosan-

treated plants and was 21.6 times higher than that of control plants (0.30 ± 0.12 ΔOD/min·mg protein) with p-value of 0.047.

The result was similar for chitinase activity. Before the treatment, chitinase activity of pre-treatment exudates were relatively comparable between control (1.67 ± 0.51 mmol GlcNAc released per g protein) and chitosan groups (1.34 ± 0.33 mmol GlcNAc released per g protein). After the treatment, the activity increased to 2.02 ± 0.89 mmol GlcNAc released per g protein in chitosan group but dropped to 0.28 ± 0.02 mmol GlcNAc released per g protein in the control. The difference was approximately 7.2 times but statistical test (T-test) showed no significant difference with a p-value of 0.12 between these comparisons due to high variation among the three replicates of chitosan group, which displayed a coefficient of variation (CV) = 76.13%.

After being treated with colloidal chitosan for 7 days, peroxidase and chitinase activities measured from the root of chitosan-treated plants were 2.3 and 1.7 times higher than those of control plants. The differences were much stronger in root exudates as peroxidase and chitinase activities were 21.6 and 7.2 times higher in chitosan group. This implies that plants produce more peroxidase and chitinase enzymes in root tissues and secrete them out into the exudate in response to chitosan treatment. By contrast, peroxidase and chitinase activities were not different between the shoots of control and chitosan-treated plants. This could be because chitosan had a localized impact on protein expression where plant roots were directly exposed to chitosan but the effect did not transfer to aboveground tissues.

Table 2
Total protein concentration and enzymatic activities of peroxidase and chitinase from shoot and root tissues of control and chitosan-treated plants.

Plant tissue	Condition	Protein content (mg protein/g fresh weight)	Peroxidase activity (ΔOD/min·mg protein)	Chitinase activity (mmol GlcNAc released/g protein)
Shoot	**Control**	13.62 ± 1.26	0.51 ± 0.12	0.21 ± 0.02
	Chitosan	10.88 ± 2.96	0.66 ± 0.11	0.21 ± 0.04
Root	**Control**	2.72 ± 0.33	13.17 ± 0.80	0.51 ± 0.20
	Chitosan	1.27 ± 0.46	30.80 ± 8.06‡	0.85 ± 0.11

Values express mean ± SEM from three biological replicates. ‡ 0.05 < p-value < 0.10 (T-test), comparing between control and chitosan conditions.

Table 3
Total protein concentration and enzymatic activities of peroxidase and chitinase from root exudates of control and chitosan-treated plants.

	Condition	Protein content (µg protein/ml retentate)	Peroxidase activity (ΔOD/min·mg protein)	Chitinase activity (mmol GlcNAc released/g protein)
Pre-treatment	Control	53.80 ± 11.91	0.13 ± 0.04	1.67 ± 0.51
	Chitosan	81.07 ± 16.99	0.04 ± 0.01	1.34 ± 0.33
Post-treatment	Control	146.20 ± 15.52	0.30 ± 0.12	0.28 ± 0.02
	Chitosan	104.87 ± 11.14	6.48 ± 2.17*	2.02 ± 0.89

Values express mean ± SEM from three biological replicates. * p-value < 0.05 (T-test), comparing between control and chitosan conditions.

Phytohormone content

Phytohormones play a crucial role in plant defense from biotic stresses caused by living organisms including herbivores, insects, bacteria, fungi and viruses [36]. Salicylic acid (SA), jasmonic acid (JA) and ethylene (ET) are on the front line of combat, functioning as signal molecules once a plant detects pests and/or pathogens. Other hormones such as abscisic acid (ABA), auxins, cytokinins, gibberellins and brassinosteroids, typically associated with plant growth and abiotic stresses, are induced later through interactions with SA, JA and ET signaling networks [37]. This study aimed to verify whether challenging industrial hemp with exogenous chitosan modulates the production of plant hormones. Targeted metabolomics approach using a liquid chromatography-mass spectrometry (LC-MS) machine coupled with multiple reaction monitoring (MRM) detection mode was employed to quantify phytohormones levels in shoot and root tissues. Zeatin, indole-3-acetic acid (IAA) and brassinolide (BL) were detected as representatives of cytokinin, auxin and brassinosteroid phytohormone classes, respectively. In addition to major hormones, JA derivatives, jasmonyl-isoleucine (JA-Ile) and 12-oxo-phytodienoic acid (OPDA) and cinnamic acid (CA), a growth-stimulating compound [38] were also analyzed.

Phytohormone levels varied in a wide range from 14.10 ± 0.79 ng of IAA to 35.76 ± 12.62 mg of OPDA per 1 g tissue FW. Zeatin and BL were undetectable in all samples. All quantifiable phytohormones were found to be higher in shoots (Table 4). For example, JA and JA-Ile were only observed in plant shoots. SA content in the shoot of control plants (5888.00 ± 2416.20 ng/g FW) was approximately 250 times higher than that in the roots (23.85 ± 8.92 ng/g FW). When comparing overall phytohormone content between control and chitosan conditions using principal component analysis (PCA), shoot samples of both groups were clearly separated from each other in the score plot of the first two components (Additional file 4). This indicates that treating plants with chitosan affects phytohormone production in this plant system. An approximately 10-fold difference was found between the shoots of control (5888.00 ± 2416.20 ng/g FW) and chitosan-treated plants (608.53 ± 39.42 ng/g FW) for SA. The levels of JA, JA-Ile, OPDA and CA

were approximately 2–6 times higher in control plants. The observed lower concentrations of phytohormones in shoot tissues of chitosan-treated plants may be due to a reduction of plant growth caused by the 1% w/v colloidal chitosan. As noted from morphological data, root development was impeded after chitosan was introduced on day 7. Although decreased growth was not observed in shoot tissues, adaptation responses are likely shared between the above and below ground plant tissues in this system.

The levels of phytohormones were comparable in the root tissues between control and chitosan-treated plants (Table 4). The PCA plot did not demonstrate clear separation between both groups (Additional file 4). For instance, SA contents were 23.85 ± 8.92 and 18.73 ± 2.76 ng/g FW for control and chitosan-treated plants, respectively. OPDA, IAA and CA contents were slightly higher in chitosan condition. However, concentration of ABA was significantly higher in chitosan group (170.55 ± 6.82 ng/g FW) relative to control (96.62 ± 4.69 ng/g FW) with p-value at 0.0001. Increasing amount of ABA under chitosan condition would be correlated to lesser root development in chitosan-treated plants. ABA has been reported to inhibit lateral root formation in *A. thaliana*, pea and tomato [39, 40]. However, the overall effect of ABA on plant root formation is diverse depending on ABA concentration, plant age and environmental factors [41]. ABA also interacts with auxin and ethylene signaling pathways in controlling plant root growth [42], hence it is difficult to predict a direct effect of ABA in the root system [43]. Conversely, unchanged levels of other hormones would be a consequence of bilateral effect of chitosan on root tissues. Cellular phytohormones might be produced less because of reduced root development. On the contrary, the plants might modulate defense signaling pathways in response to chitosan recognition, leading to a rebound of overall phytohormone contents in the root system. However, this is an early assumption and requires further investigation to confirm the effect of chitosan on phytohormone contents in root tissues.

The difference of phytohormone levels between control and chitosan-treated plants was more obvious when comparing the proportions between roots and shoots (Table 4). Root-to-shoot ratios of all detected phytohormones were significantly higher in chitosan condition as compared to the control. This result pinpoints that plants respond towards exogenous chitosan treatment through phytohormone production.

Table 4
Phytohormone contents detected from shoot and root tissues of control and chitosan-treated plants.

	Phytohormone contents (ng/g fresh weight)					
	Control			Chitosan		
	Shoot	Root	Root/shoot ratio	Shoot	Root	Root/shoot ratio
SA	5888.00 ± 2416.20	23.85 ± 8.92	0.004 ± 0.001	608.53 ± 39.42	18.73 ± 2.76	0.030 ± 0.003*
JA	205.67 ± 92.80	N.D.	N.D.	34.56 ± 1.55	N.D.	N.D.
JA-Ile	272.50 ± 116.29	N.D.	N.D.	51.09 ± 11.65	N.D.	N.D.
OPDA	35758.87 ± 12622.87	8552.14 ± 2732.78	0.26 ± 0.02	15586.85 ± 3799.29	13053.10 ± 4101.16	0.79 ± 0.07*
ABA	716.94 ± 129.09	96.62 ± 4.69	0.15 ± 0.03	478.62 ± 85.24	170.55 ± 6.82*	0.41 ± 0.10*
IAA	21.70 ± 1.25	14.43 ± 1.46	0.67 ± 0.08	14.06 ± 0.79*	16.82 ± 1.52	1.22 ± 0.17*
CA	259.48 ± 23.90	47.73 ± 8.48	0.16 ± 0.03	44.88 ± 4.61*	55.28 ± 2.39	1.19 ± 0.13*
Zeatin	N.D.	N.D.	N.D.	N.D.	N.D.	N.D.
BL	N.D.	N.D.	N.D.	N.D.	N.D.	N.D.

Values express mean ± SEM from three biological replicates. N.D.; not detectable. * p-value < 0.05 (T-Test), comparing between control and chitosan conditions within same type of plant tissues.

Nucleic acid extraction and gene detection

Plant defense-related genes such as chitinases are key targets for determining gene expression in response toward chitosan treatment [44, 45]. These genes have not been characterized but only computationally predicted from the assembly of *C. sativa* draft genome [46]. The genome was constructed from medicinal cannabis Purple Kush variety and industrial hemp Finola and USO-31 strains. The first step of molecular detection in this study was to ensure that target genes are detectable from the studied industrial hemp (Ferimon variety) and chitosan does not interfere with any steps of nucleic acid extraction. DNA was extracted from shoot and root tissues of control and chitosan-treated plants. Primers of all genes were designed based on the *C. sativa* draft genome using the NCBI primer-BLAST tool [47]. Actin, ubiquitin and elongation factor-1 alpha (EF-1α) were selected as reference genes. Three chitinase isoforms, chitinase 5, chitinase 2 and chitinase 4-like were selected as primary targets for monitoring DNA analysis. Gene information and primer details are supplied in Additional file 5. Traditional PCR method coupled with ethidium bromide staining was used to analyze DNA amplification products.

Before undertaking PCR reactions, DNA from all samples were measured and normalized to 100 ng/µl. As shown in Fig. 6, amplification and detection of all target genes was achieved in both shoot and root samples. In root tissues, amplicons of actin, ubiquitin and EF-1α genes were relatively comparable between control and chitosan-treated plants. In shoot tissues, the third control replicate showed slightly lesser DNA copies than the first two replicates for all genes. PCR bands of EF-1α detected from the shoots of chitosan-treated plants were slightly denser than those of controls, suggesting EF-1α would not be an ideal reference gene for quantitative analysis. The levels of chitinase 5, chitinase 2 and chitinase 4-like genes were relatively comparable between control and chitosan-treated plants in both shoot and root tissues (Fig. 6). Since chitosan has been reported to bind with nuclear chromatin and damage DNA structure in pea [48], these PCR results showed that chitosan does not impair the process of nucleic acid extraction or amplification.

Future directions for gene analysis include implementing quantitative PCR methods such as real-time and digital PCR to investigate gene expressions at transcription level (RNA) to explore the molecular effects of chitosan. Other genes involving in plant defense system, for instance mitogen-activated protein kinase (MAP kinase), catalase and glucanase will be included to extend the understanding of chitosan effect on plant defense-related genes.

Discussion

Root-TRAPR system - a new plant cultivation device based on the EcoFAB model

In this study, we have developed Root-TRAPR system, a modified EcoFAB device which is larger in size, modular, reusable, and easy to fabricate. The system is designed to accommodate the largest microscope slide available (128×85 mm) and to suit industrial hemp, an economic crop that grows to a larger size as compared to model plants. The PDMS gasket is sandwiched between a bottom microscope slide and acrylic top sheet. They are enclosed within a 3D-printed PLA frame, secured with nylon bolts and nuts. In comparison to the original EcoFAB model [9], Root-TRAPR system does not require a plasma chamber to bond the microscope slide with a cast PDMS root growth chamber. The system can be cleaned and reused to reduce unnecessary lab waste generation. The frame and other 3D objects can be manufactured using any type of 3D printer and the design files provided in Additional files 6–11 are in a standard STL file format. All other materials such as acrylic sheet, nylon screw, and rubber stopper are accessible from general hardware stores.

Additionally, printing materials can be substituted with other types of 3D printing plastic such as polyetherimide (PEI) and polyether ether ketone (PEEK) which are highly robust, temperature insensitive and chemically inert [49, 50]. However, these materials are significantly more expensive. The PDMS gasket which we manually cast in a 3D-printed mold can also be simply created using advanced 3D printing technology such as PolyJet printer which is compatible with a wide range of resin materials including rubber-like and polypropylene-like photopolymers [51]. The modular nature of Root-TRAPR

system allows for different sized gaskets, which enables fine tuning of the growth chamber volume by increasing or decreasing the gasket oval diameters and/or the gasket thickness. This can be achieved by redesigning specific molds or directly printing different sizes of the gasket. Glass microscope slides can be replaced by an identical-sized plastic acrylic sheet in scenarios where examination of root microanatomy or microbe localization using microscopes is not required for instrumental analysis. In addition, other types of transparent plastic such as polycarbonate (PC) sheet can be used to replace any top or bottom layer.

As shown in the results, root morphology of the plants grown in Root-TRAPR system can be directly observed using a root scanner (Fig. 3). Collection of root exudates in small volumes is achievable and can be promptly processed to extract proteins in a single step of centrifugation. The plant shoot and underground parts can be readily collected from the model and subjected to instrumental analyses for examining plant biochemical responses. Root-TRAPR system can be applied to a range of other plant physiological studies, for instance elucidating mechanisms of plant nutrient uptake, investigating plant stress responses in different environments, and exploring plant-microbe interactions occurring underground. However, the system requires specific environmental conditions to maintain sterile conditions prior to use for microbial observations. When grown in the current Root-TRAPR system, plants are exposed to an open space and could be contaminated by surrounding microorganisms, thereby interfering with the experiment. To establish a closed system, experiments may be conducted in dedicated growth chambers or within a light transparent sterile box to house the whole plant-inside-Root-TRAPR unit. Sterile conditions will also facilitate further investigation of mechanisms underlying fungal infections in *C. sativa* plants and the effect of chitosan treatment after the plants are already affected by pathogens.

Chitosan effect on industrial hemp

Chitosan is a well-known plant biostimulant, used for stimulating plant growth, inducing plant abiotic stress tolerance, and enhancing plant pathogen resistance [24, 25]. The compound has been recorded to benefit a wide variety of agricultural crops in different ways [52]. For example, seed soaking in chitosan solution prior to sowing can increase production of antioxidant compounds in sweet basil [53]. In tomato, foliar spraying with chitosan can promote crop yield and reduce the severity of bacterial and fungal infections [54]. Post-harvest coating of mango fruits with edible chitosan can prolong shelf-life by delaying progression of microbial diseases [55]. However, mechanisms underlying beneficial effects of chitosan have remained unclear [56]. Although chitin, an acetylated form of chitosan, can bind to specific receptors such as chitin elicitor receptor kinases (CERKs) and chitin elicitor binding proteins (CEBiPs) on plant cell membranes to trigger overall plant immunity [57], chitosan has low affinity to those receptors and does not induce any signaling cascades in plant immune pathways [58, 59]. Based on current understanding, challenging plants with chitosan enhances cellular levels of secondary messengers, H_2O_2 and nitric oxide (NO) as well as phytohormones including ABA, JA and SA, and eventually manipulates expressions of defense-related genes inside the nucleus [60]. Changes may lead to increased production of antioxidant compounds and catalytic enzymes such as catalase, chitinase, peroxidase, superoxide

dismutase, and phenylalanine ammonia-lyase [52]. Apart from enhancing cellular defense mechanism, chitosan can also induce the secretion of plant defense molecules including phytohormones and phenolic acids into an extracellular space or exudate [61].

Our findings on industrial hemp are consistent with a benefit of chitosan on plant defense. Two significant plant defense enzymes, chitinase and peroxidase, and phytohormones were monitored in this study. After treating plant roots with 1% w/v colloidal chitosan for a week, peroxidase and chitinase activities increased in root tissues and exudate (Tables 2 and 3). The increases were more intense in root exudate being 21- and 7-times higher than the control, respectively. In contrast, root tissues showed only approximately 2-times increases for both enzymes. It is possible that enzymes in root induced by chitosan are secreted into the rhizosphere to add another layer of protection for the plant. However, peroxidase and chitinase activities remained unchanged in the shoots. This suggests that chitosan may affect plant biology at local sites of exposure as only the root tissue was directly exposed to chitosan. The effect was not observed to be transferable to other distant parts of the plant, as the shoot showed no difference in enzymatic activities.

Furthermore, chitosan reduced the amount of phytohormones quantified in shoot tissues but did not change that of root system (Table 4). Lower levels of hormones in the shoots would be correlated to plant growth which tended to slow down after exposure to high concentration of chitosan. The observation of increased levels of ABA in root tissues of chitosan-treated plants appears correlated to an underproduction of branch roots [39]. The root-to-shoot ratio of all phytohormones were higher in chitosan condition. This might be because an inducing effect of chitosan to promote production and/or accumulation of plant defense hormones in the root system. Increased levels of plant defense hormones such as SA and OPDA could crosstalk with other hormonal signaling pathways [62], thereby activating biosynthesis of other hormones and balancing their levels in the root cells. Nonetheless, this is an early observation from the quantitative data and requires further exploration and additional perspectives from proteomics or transcriptomics to comprehensively verify the outcome.

Gene detection was also conducted in this study to initiate PCR methods for future gene expression analysis on plant defense-related genes. Three chitinase genes including chitinase 5, chitinase 2 and chitinase 4-like were successfully amplified using the primers designed from the *C. sativa* draft genome sequence [46]. Potential reference genes including actin, ubiquitin and EF-1α were all detectable. This result indicates reliability of the draft genome to be used as a template for designing primers and studying gene analysis on different *C. sativa* cultivars.

This research has also optimized and established an experimental workflow for exploring biological responses of *C. sativa* towards exogenous stimuli (Fig. 7). The protocol is straightforward but comprehensive, combining three analytical approaches including genomics, metabolomics and enzymatic assays to understand plant responses from different perspectives. The workflow is not only limited for studying plants grown in Root-TRAPR system but applicable for using with plants grown in the original EcoFAB device, normal hydroponic setup or other plant-growing systems. Other plant

pathogenesis-related proteins, for example catalases, glucanases, superoxide dismutases and thaumatin-like proteins should be included in further studies to add further depth to the current findings.

Furthermore, experiments in this study were conducted using three biological replicates to demonstrate and test the reproducibility of Root-TRAPR system as an alternative platform for growing *C. sativa* plants and collecting samples to perform analytical measurements. The results demonstrate that the samples harvested from Root-TRAPR systems can be successfully used for plant physiological and biological analyses, meeting our main objective. However, higher replication of plant numbers should be considered for future experiments to address the high variation observed in this study. The observed variation is likely to reflect the inherent biological variability of industrial hemp seeds, Ferimon variety, that were used in this study. Ferimon is a cropping seed-type cultivar and not generally used for research purposes.

Finally, the effect of chitosan has not been reported on *C. sativa*, in either industrial hemp or medicinal cannabis cultivars. This is the first study showing that chitosan has a potential to trigger defense system of cannabis plants. When applying to the fields, this could benefit agriculture in both industrial hemp and medicinal cannabis sectors because they are affected by the same pests and pathogens. However, before being introduced into a disease management scheme, the result needs to be verified in a large-scale production and on actual agricultural sites. The effect of chitosan also varies upon its concentration and formulation. We have found that 1% w/v colloidal chitosan forms a highly viscous mixture which could be a reason of plant root development suppression, and this would probably diminish plant yield when applying to the field. Hence, further study is essential to monitor chitosan effects at lower concentrations to identify the best that can preserve chitosan benefit whilst maintaining optimal plant growth. Assessing chitosan effects at later stages of plant development such as budding, flowering and seed-setting stages would also be worthwhile. In summary, chitosan is an inexpensive resource and readily available from by-products of the seafood industry [63], hence it could be a potential elicitor to help counteract fungal diseases in agriculture.

Conclusion

In this research, Root-TRAPR system has been developed for growing larger plants under *in vitro* conditions. The system was tested using an industrial cropping cultivar of *C. sativa*, then exploring the impact of chitosan, a potential defense elicitor molecule on plants. The system enabled the visualization of root material and the ability to harvest plant tissues and exudates, that were then successfully processed for enzymatic activity assays, phytohormone measurements and nucleic acid extraction. After treating the plants with 1% w/v chitosan for seven days, chitinase and peroxidase activities were promoted in root tissues and exudates. This confirms the effect of chitosan to induce plant defense enzymes that are associated with increased disease resistance. Finally, Root-TRAPR system has opened the way for further analysis of *C. sativa* and other larger plants under defined *in vitro* conditions.

Methods

Chemicals

Analytical grade solvents (ethanol, isopropanol, hydrochloric acid, phosphoric acid) were supplied by ChemSupply, Australia. LC-MS grade solvents (acetonitrile and formic acid) were acquired from Thermo Fisher Scientific, US. Deionized water was used during plant growth experiments, whereas Milli-Q water (Merck Millipore, Germany) was used for all analytical processes. Formulation of Hoagland solution is supplied in Additional file 1.

Root-TRAPR system fabrication

Materials used for fabricating Root-TRAPR system are listed in Table 1 and the fabrication procedure is described step by step as follows.

Printing PDMS mold, external frames and supplementary parts

PDMS mold (Fig. 2e), top and bottom external structural frame (Fig. 2d), stand (Fig. 2h) and window shutter (Fig. 2i) were manufactured using a FDM 3D printer (MakerBot Replicator plus, US). All components were designed using an open-source computer-aided design (CAD) software (FreeCAD, https://www.freecadweb.org/). The design files are supplied in Additional files 6–11. Infill was set at 80% for external structural frame and 10% for PDMS mold, stand and window shutter. The objects were printed on a raft base layer with a light fill support underneath. Layer height was set at 0.2 mm with 2 shells. After printing, the internal surfaces of the PDMS mold were finished with coarse (P80) and fine (P600) sandpapers. Printing scrap and support were removed from all printed items prior to use.

Casting PDMS gasket

A Sylgard 184 elastomer kit (Dow Corning, US) was used to create the PDMS gasket. Standard 10:1 (w/w) ratio of base to catalyst was used. Eighteen g of silicone base was mixed with 1.8 g of curing agent in a disposable foil baking cup. The mixture was placed in a vacuum chamber for 30 min to remove air bubbles and then gently poured into the 3D-printed PDMS mold. Overfill was removed by scraping a ruler across the top surface of the mold. The filled mold was incubated at 55°C overnight to allow the elastomer to set. The solidified PDMS gasket was slowly cut away from the mold using a single edge razor blade. Completed PDMS gasket is shown in the middle of Fig. 2c.

Preparation of the upper viewing window acrylic sheet

An acrylic sheet was cut into a desired size (128×85 mm) using a Felder BF-5 combination machine (Felder Group, Austria). Then two circular holes were added using a drill press with appropriately diameter sizes of 8- and 9-mm bits. The upper larger hole (9 mm) is left blank for placing the seed, while the lower smaller hole (8 mm) was firmly stoppered with a rubber bung (Fig. 2g) to stop leakage. Completed acrylic sheet is presented on the left of Fig. 2c.

Assembly of Root-TRAPR unit

The completed Root-TRAPR system was assembled by placing the PMDS gasket between a microscope glass slide underneath and an acrylic sheet atop. The three internal components were then positioned inside the pocket of the bottom external frame and enclosed by the top frame. Finally, eight sets of pre-sized nylon bolts and nuts (Fig. 2f) were screwed in to tighten the layers and complete the main assembly. Additionally, during growth experiments the stand (Fig. 2h) and window shutter (Fig. 2i) can be incorporated to tilt the model at a 25° angle from the ground to promote gravitropism and to prevent direct light onto the plant root, respectively.

Sterilizing Root-TRAPR system

Before use, the assembled Root-TRAPR system and supporting parts were placed in a plastic container and submerged in 70% ethanol for 30 min and 100% ethanol for another 10 min. It was shaken occasionally to ensure all parts exposed to the solvent and the oval root growth chamber was filled throughout. After sterilization, the solvent was drained off and the model was dried in a laminar flow cabinet. Once seedlings had germinated, the sterilized Root-TRAPR system was rinsed with autoclaved deionized water and filled with 15 ml of full-strength Hoagland solution.

Colloidal chitosan preparation

Colloidal chitosan was prepared according to previous method [64] with a slight modification. Five g of chitosan powder (medium molecular weight; Sigma, US) was first mixed with 50 ml of 85% phosphoric acid, followed by slowly adding another 50 ml of the acid with continuous stirring. The mixture was left at 4°C overnight to form a colloidal suspension. Pre-cooled 500 ml of 50% ethanol was added to dilute the mixture, then left at 4°C overnight again. The suspension was filtered through Whatman Grade 1 filter paper (Whatman plc, UK) aided by vacuum filtration. Colloidal chitosan was retained in the funnel and then washed with distilled water until pH above 5. The retentate was transferred to 50-ml conical tubes and then lyophilized in an Alpha 1–4 LD plus freeze-drier (Christ, Germany). Before use, dried chitosan was resuspended to 1% w/v in Hoagland solution.

Seed germination

Overview of experimental workflow starting from seed germination until sample collection is illustrated in Fig. 7. Industrial hemp seeds, Ferimon (France) was received from Southern Hemp Australia. Obtaining and processing industrial hemp (low-THC cannabis) at the University of Melbourne is authorized by Agriculture Victoria, the State Government (authority number 2019/12). The seeds were sterilized with 70% ethanol for 1 min and 0.04% sodium hypochlorite for 10 min, followed by rinsing 3 times with autoclaved deionized water. Sterile seeds were imbibed at room temperature overnight and transferred to round petri dishes (90 mm in diameter) containing moistened filter paper. Germination was conducted in the dark at ambient temperature (approximately 20°C) for three days. Day 0 was counted when the seedlings were transferred into Root-TRAPR system.

Plant growth and chitosan treatment

Seedlings with 4–6 cm-long tap root were transferred to Root-TRAPR systems supplied with 15 ml of Hoagland solution using sterilized forceps. Plants were maintained for seven days in a CMP6010 growth chamber (Conviron, Canada) at 25°C for 16 h with light and at 21°C for 8 h of darkness. Light intensity was set at level 2 and relative humidity was maintained at 60%. Nutrient solution was filled up every 2–3 days to compensate liquid consumption and evaporation. On day 7, plants were separated into two groups – control and chitosan conditions. In control group, the entire solution was collected and substituted with a new 15 ml of Hoagland solution. In chitosan group, pre-treated solution was collected and replaced with 1% w/v colloidal chitosan suspension. All plants were maintained under the same condition for another seven days. Hoagland solution (approximately 1–2 ml) was added up every 2–3 days in both groups for liquid compensation.

Root growth measurement

Root growth was monitored and analyzed under a well-calibrated root scanning system which is composed of an optical scanner (Epson Perfection V800, Japan) equipped with WinRHIZO Arabidopsis 2019 software (Regent Instruments, Canada). Plant roots were scanned every 2–3 days by placing the Root-TRAPR device straight on the document table of the scanner and leaving the lid open. Root measurement was determined in three different parameters – root length, root surface area and average root diameter. Root region was automatically detected by the software in a greyscale mode. Root was set brighter than background. Manual adjustment was carried out when root region was misread by the automatic detection. Root analysis was performed under standard precision and normal cross detection. Additionally, plant shoot and overview plant structure were photographed using a smartphone camera (Xiaomi Redmi 5, China).

Plant tissues and root exudate collection

Plant shoot and root tissues were harvested on the last day of observation. Plant shoot included stem and leaves sitting above the node of the cotyledons. Plant root was assigned to all parts developing under Root-TRAPR root growth chamber. They were ground using mortar and pestle under freezing conditions of liquid nitrogen. Fine tissue powder was separately transferred to three micro-centrifuge tubes in an approximate 100 mg by weight (Fig. 7). The tubes were weighed and stored in a -80°C freezer until further use.

Root exudate was collected twice on day 7 (pre-treatment) and day 14 (post-treatment). It was drawn from the Root-TRAPR root growth chamber into a 50-ml conical tube. The solution was spun at 2,500 ×g, 4°C for 20 min to remove debris. Supernatant was transferred to a 10 kDa molecular weight cutoff (MWCO) Amicon Ultra-15 centrifugal filter unit (Merck Millipore, Germany) and then centrifuged at 4,000 ×g, 4°C for 40 min to concentrate root exudate proteins. Approximately 200 µl of protein fraction was captured in the filter unit and stored at -80°C until further use.

Biological assays

For tissue samples (shoot and root), 1 ml of 100 mM phosphate buffer, pH 6.5 was added to extract proteins from tissue powder (approximately 100 mg). The tube was vortexed and centrifuged at 13,000 ×g for 20 min. Supernatant was collected and stored at -20°C until assay. For root exudate, concentrate protein (approximately 200 µl) was straightaway assayed as follows.

H_2O_2 detection

Working solution of titanium tetrachloride ($TiCl_4$) was pre-made by slowly adding 100 µl of concentrated $TiCl_4$ solution (product code: 208566, Sigma, US) to 100 µl of 6 M hydrochloric acid (HCl) on ice. The mixture was left at 4°C overnight and then diluted in 10 ml of 6 M HCl.

Twenty µl of tissue extract was mixed with 80 µl of 100 mM phosphate buffer, pH 6.5 in 96-well microplate. Immediately before detection, 100 µl of working $TiCl_4$ solution was added into each well. Absorbance was measured at 415 nm using an EnSpire Multilabel plate reader (PerkinElmer, US). H_2O_2 content was calculated against a calibration curve, created from serial dilutions of 0.001–0.05% v/v standards.

Protein measurement

Bradford reagent (Bio-Rad, US) was diluted 5 times in deionized water. A 20 µl of protein extract was mixed with 180 µl of diluted Bradford reagent in 96-well microplate. The mixture was incubated at room temperature for 10 min. Absorbance was detected at 595 nm using the plate reader. Protein concentration was measured against a bovine serum albumin (BSA) standard curve (0-100 µg/ml).

Peroxidase activity

Twenty µl of protein extract was mixed with 150 µl of 0.025% H_2O_2, diluted in 100 mM phosphate buffer, pH 6.5 in 96-well microplate. Immediately before assay, 50 µl of 50 mM guaiacol was added into the solution. Absorbance was measured at 470 nm and repeated every 30 s. Rate of absorbance change on the first 3 min was calculated to represent guaiacol peroxidase activity in a unit of ΔOD/min, normalized to protein amount.

Chitinase activity

Dimethylaminobenzaldehyde (DMAB) stock solution was prepared by dissolving 8 g of DMAB pellet in a mixture of 70 ml of glacial acetic acid and 10 ml of 32% HCl. Before the assay, working DMAB solution was prepared by diluting the stock solution 10 times in glacial acetic acid.

Forty µl of protein solution was mixed with 100 µl of 1% w/v of colloidal chitin [65], suspended in 50 mM acetate buffer, pH 5.5 and then incubated at 37°C for 2 h. The reaction was stopped by centrifugation at 8,000 ×g for 10 min. Forty µl of 1 M sodium borate buffer, pH 8.5 was added into a mixture, then incubated at 95°C for 5 min and cooled on ice for 20 min. Five hundred µl of working DMAB reagent was added into a solution, then incubated at 37°C for 20 min. Final solution was aliquoted into a 96-well

microplate and detected at 585 nm. Chitinase activity was evaluated against GlcNAc standard curve (0.02-2 mM) and expressed as mmole GlcNAc released per 1 g protein.

Phytohormone measurement

Phytohormones were extracted from tissue powder using 200 µl of 70% methanol supplied with 500 ng/ml of internal standards (d_5-zeatin, d_2-IAA, d_7-CA, d_4-SA, d_6-ABA and H_2JA). Samples were vortexed and centrifuged at 13,000 ×g for 20 min. Supernatant was transferred into a glass LC-MS vial containing an insert and injected to 1200 series LC system equipped with 6410 Triple Quadrupole MS machine (Agilent, US). Metabolites were separated on Eclipse XDB-C18, 1.8 µm, 2.1×100 mm column (Agilent, US). Column temperature was set at 45°C. Mobile phase A and B were 0.1% formic acid in water and acetonitrile, respectively. The elution gradient was set as follows: 80% A (0–2 min), 80 – 50% A (2–3 min), 50 – 5% A (3–12 min), 5% A (12–16 min), 5–80% A (16–17 min) and 80% A (17–23 min). Flow rate was 320 µl/min and injection volume was 5 µl. Analytes were ionized using electrospray ionization (ESI) source with capillary voltage at 5500 V and 4500 V for positive and negative modes, respectively. Nebulizer was set at 55 psi. Nitrogen gas flow was maintained at 13 L/min and 250°C. Phytohormones were detected using multiple reaction monitoring (MRM) program according to the published method [66]. The MRM transitions, collision energies and polarities were applied as follows: zeatin (220.1 ◊ 136.1 *m/z*, 14 eV, positive), IAA (176.1 ◊ 130.1 *m/z*, 10 eV, positive), CA (149.1 ◊ 103.1 *m/z*, 20 eV, positive), BL (481.5 ◊ 315.3 *m/z*, 10 eV, positive), SA (137.0 ◊ 93.0 *m/z*, 16 eV, negative), ABA (263.1 to 153.1 *m/z*, 8 eV, negative), JA (209.1 ◊ 59.0 *m/z*, 8 eV, negative), JA-Ile (322.1 ◊ 129.9 *m/z*, 24 eV, negative), OPDA (291.0 ◊ 164.9 *m/z*, 20 eV, negative), d_5-zeatin (225.2 ◊ 137.1 *m/z*, 20 eV, positive), d_2-IAA (178.1 ◊ 132.0 *m/z*, 12 eV, positive), d_7-CA (156.1 ◊ 109.0 *m/z*, 22 eV, positive), d_4-SA (141.0 ◊ 97.1 *m/z*, 16 eV, negative), d_6-ABA (269.1 ◊ 159.1 *m/z*, 8 eV, negative) and H_2JA (211.1 ◊ 59.0 *m/z*, 12 eV, negative). Phytohormone concentrations were measured by comparing relative peak area against calibration curves, created from serial dilutions of the standards. The curve was plotted from 4–6 data points in a range of 10-1000 ng/ml according to the phytohormone levels found in the samples.

DNA extraction and PCR analysis

Four hundred µl of DNA extraction buffer (160 mM Tris, 56 mM EDTA, 30 mM sodium metabisulfite and 1.6 M sodium chloride) was added into tissue powder (approximately 100 mg) and centrifuged at 13,000 ×g for 5 min. Three hundred µl of supernatant was taken and mixed with 300 µl of 100% isopropanol. The mixture was incubated at room temperature for 10 min with occasionally tube-inverting and then centrifuged at 13,000 ×g for 5 min. The pellet was washed with 300 µl of 70% ethanol and air-dried overnight. Dried DNA pellet was dissolved in 50 µl of nuclease-free water (Qiagen, Germany). DNA concentration was measured using UV5Nano spectrophotometer (Mettler-Toledo, US).

Six *C. sativa* genes (encoding actin, ubiquitin, EF-1α, chitinase 5, chitinase 2 and chitinase 4-like) were predicted from the *C. sativa* draft genome [46]. Gene and primer details are described in Additional file 5. A 100 ng of DNA template was added to 25 µl of PCR reaction mixture, consisted of 1× MyTaq Red buffer, 0.5 U MyTaq DNA polymerase (Bioline, US) and 0.4 µM forward and reverse primers each. The PCR

amplification was performed using T100 thermal cycler (Bio-Rad, US) with an initial denaturation of 2 min at 95°C, following by 35 cycles of 30 s at 95°C, 30 s at 55°C and 1.15 min at 72°C, and a final extension of 5 min at 72°C. A 10 µl of amplification product was resolved in 1% agarose gel electrophoresis at 85 V for 50 min. The gel was stained with ethidium bromide and analyzed using Gel Doc EZ imager equipped with ImageLab software (Bio-Rad, US).

Statistical analysis

Two-tailed student's T-test was used for enzymatic activity and phytohormone content with Microsoft Excel 2016 software. One-way ANOVA followed by Tukey's honestly significant difference (HSD) analysis was used for root growth measurement and hydrogen peroxide content with Minitab 19 software. A p-value below 0.05 was considered as a significant difference between tested conditions. P-value above 0.05 but below 0.10 was marginally significant difference. Online MetaboAnalyst 5.0 software [67] was used to perform principal component analysis (PCA) of overall phytohormone content. Before the analysis, Pareto data scaling was employed to normalize shoot tissue data while the data of root tissue was log-transformed and scaled using mean centering.

Abbreviations

3D: three-dimensional, ABA: abscisic acid, ANOVA: analysis of variance, BL: brassinolide, CA: cinnamic acid, DMAB: dimethylaminobenzaldehyde, EcoFAB: ecosystem fabrication, EDTA: ethylenediamine-tetra-acetic acid, EF-1α: elongation factor-1 alpha, FDM: fused deposition modelling, FW: fresh weight, GlcNAc: *N*-acetylglucosamine, H_2O_2: hydrogen peroxide, HCl: hydrochloric acid, HSD: honestly significant difference, IAA: indole-3-acetic acid, JA: jasmonic acid, JA-Ile: jasmonyl-isoleucine, LC: liquid chromatography, MRM: multiple reaction monitoring, MS: mass spectrometry, OD: optical density, OPDA: 12-oxo-phytodienoic acid, PCA: principal component analysis, PCR: polymerase chain reaction, PDMS: polydimethylsiloxane, PLA: polylactic acid, Root-TRAPR: root-transparent, reusable, affordable three-dimensional printed rhizo-hydroponic, SA: salicylic acid, SEM: standard error of the mean, THC: tetrahydrocannabinol, $TiCl_4$: titanium tetrachloride

Declarations

Authors' contributions

PS, RW and BAB designed and planned the study. PS conducted the experiments and analyzed the data. RW, AI, JSP and BAB provided guidance and technical support throughout the study. PS prepared the manuscript. PS, RW, AI, JSP and BAB edited and approved the final version.

Authors details

[1]School of BioSciences, University of Melbourne, Victoria 3010, Australia. [2]Nutrifield Pty Ltd, Victoria 3020, Australia. [3]Australian National Phenome Centre, Murdoch University, Western Australia 6150, Australia.

Acknowledgements

We thank David Brian from Southern Hemp and Ken Stuckey from Leawood Hemp for supplying industrial hemp seeds, Michael Zammit from Science Workshop, University of Melbourne for preparing acrylic sheets, and Gary Mather from Engineering Workshop and Eric Jong from Research Computing Service Training at the University of Melbourne for providing training and suggestion on 3D printing techniques. We also thank teams in the 3D Innovation Centre, Faculty of Engineering and Information Technology, and the New Experimental Technology Lab (NExT Lab), Melbourne School of Design for assisting 3D printing. Joshua Heazlewood and Ute Roessner provided suggestions on experimental workflow.

Competing interests

The authors declare that they have no competing interests.

Availability of data and material

All data generated from this study are included in this published article and supporting materials. Additional details on Root-TRAPR fabricating procedures can be acquired from corresponding authors upon reasonable request.

Consent for publication

All authors have read and agree to publish the paper.

Ethics approval and consent to participate

Not applicable.

Funding

This study was funded by School of BioSciences Seed Funding for 2019 (SEED19), University of Melbourne. AI had support from the Australian Research Council (LP170100548). PS received a Melbourne Research Scholarship (University of Melbourne) and additional project funding through Nutrifield Pty Ltd.

References

1. Ryan PR, Delhaize E, Watt M, Richardson AE. Plant roots: understanding structure and function in an ocean of complexity. Ann Bot. 2016;118(4):555–9.
2. Taylor HM, Upchurch DR, McMichael BL. Applications and limitations of rhizotrons and minirhizotrons for root studies. Plant Soil. 1990;129:29–35.

3. Mathieu L, Lobet G, Tocquin P, Perilleux C. "Rhizoponics": a novel hydroponic rhizotron for root system analyses on mature *Arabidopsis thaliana* plants. Plant Methods. 2015;11:3.
4. Oburger E, Dell'mour M, Hann S, Wieshammer G, Puschenreiter M, Wenzel WW. Evaluation of a novel tool for sampling root exudates from soil-grown plants compared to conventional techniques. Environ Exp Bot. 2013;87:235–47.
5. Parashar A, Pandey S. Plant-in-Chip: Microfluidic system for studying root growth and pathogenic interactions in *Arabidopsis*. Appl Phys Lett. 2011;98:263703.
6. Grossmann G, Guo WJ, Ehrhardt DW, Frommer WB, Sit RV, Quake SR, et al. The RootChip: an integrated microfluidic chip for plant science. Plant Cell. 2011;23(12):4234–40.
7. Massalha H, Korenblum E, Malitsky S, Shapiro OH, Aharoni A. Live imaging of root-bacteria interactions in a microfluidics setup. Proc Natl Acad Sci U S A. 2017;114(17):4549–54.
8. Zengler K, Hofmockel K, Baliga NS, Behie SW, Bernstein HC, Brown JB, et al. EcoFABs: advancing microbiome science through standardized fabricated ecosystems. Nat Methods. 2019;16(7):567–71.
9. Gao J, Sasse J, Lewald KM, Zhalnina K, Cornmesser LT, Duncombe TA, et al. Ecosystem fabrication (EcoFAB) protocols for the construction of laboratory ecosystems designed to study plant-microbe interactions. J Vis Exp. 2018. doi:10.3791/57170(134).
10. Gao J, Northen TR, Lewald K, Cornmesser LT, Andeer PF. inventors; The Regents of the University of California, assignee. Ecosystem for determining plant-microbe interactions. US patent 10787639. 2020 September 29.
11. Sasse J, Kant J, Cole BJ, Klein AP, Arsova B, Schlaepfer P, et al. Multilab EcoFAB study shows highly reproducible physiology and depletion of soil metabolites by a model grass. New Phytol. 2019;222(2):1149–60.
12. Schluttenhofer C, Yuan L. Challenges towards revitalizing hemp: a multifaceted crop. Trends Plant Sci. 2017;22(11):917–29.
13. Valuates Reports. The global industrial hemp market to grow USD 18,812.81 million by 2025, at a CAGR of 32.17%. In: Market research reports. 360iResearch. 2020. https://reports.valuates.com/market-reports/360I-Auto-1N254/the-global-industrial-hemp. Accessed 23 April 2021.
14. Callaway JC. Hempseed as a nutritional resource: an overview. Euphytica. 2004;140:65–72.
15. Kleinhenz MD, Magnin G, Ensley SM, Griffin JJ, Goeser J, Lynch E, et al. Nutrient concentrations, digestibility, and cannabinoid concentrations of industrial hemp plant components. Applied Animal Science. 2020;36(4):489–94.
16. Gotter A. Hemp oil for skin. Healthline website. 2019. https://www.healthline.com/health/hemp-oil-for-skin. Accessed 23 April 2021.
17. Duque Schumacher AG, Pequito S, Pazour J. Industrial hemp fiber: a sustainable and economical alternative to cotton. J Clean Prod. 2020;268:122180.

18. Dhakal U, Berardi U, Gorgolewski M, Richman R. Hygrothermal performance of hempcrete for Ontario (Canada) buildings. J Clean Prod. 2017;142:3655–64.
19. AgriFutures Australia. Industrial hemp. AgriFutures Australia website. 2017. https://www.agrifutures.com.au/farm-diversity/industrial-hemp/. Accessed 23 April 2021.
20. McPartland JM, Clarke RC, Watson DP. Hemp diseases and pests: management and biological control. Oxford: CABI Publishing; 2000.
21. Punja ZK, Collyer D, Scott C, Lung S, Holmes J, Sutton D. Pathogens and molds affecting production and quality of *Cannabis sativa* L. Front Plant Sci. 2019;10:1120.
22. Punja ZK. Emerging diseases of *Cannabis sativa* and sustainable management. Pest Manag Sci. 2021. doi:10.1002/ps.6307.
23. Scott C, Punja ZK. Evaluation of disease management approaches for powdery mildew on *Cannabis sativa* L. (marijuana) plants. Can J Plant Pathol. 2020. doi:10.1080/07060661.2020.1836026.
24. Yakhin OI, Lubyanov AA, Yakhin IA, Brown PH. Biostimulants in plant science: a global perspective. Front Plant Sci. 2016;7:2049.
25. du Jardin P. Plant biostimulants: definition, concept, main categories and regulation. Sci Hortic. 2015;196:3–14.
26. Debode J, De Tender C, Soltaninejad S, Van Malderghem C, Haegeman A, Van der Linden I, et al. Chitin mixed in potting soil alters lettuce growth, the survival of zoonotic bacteria on the leaves and associated rhizosphere microbiology. Front Microbiol. 2016;7:565.
27. Olivares FL, Aguiar NO, Rosa RCC, Canellas LP. Substrate biofortification in combination with foliar sprays of plant growth promoting bacteria and humic substances boosts production of organic tomatoes. Sci Hortic. 2015;183:100–8.
28. NExT Lab. 3D printing at the NExT lab. Melbourne School of Design (University of Melbourne) website. 2021. https://msd-makerspaces.gitbook.io/next-lab/3d-printing/3dp-introduction. Accessed 23 April 2021.
29. Batubara I, Rahayu D, Mohamad K, Prasetyaningtyas WE. Leydig cells encapsulation with alginate-chitosan: optimization of microcapsule formation. JEAS. 2012;02(02):15–20.
30. Lintunen A, Paljakka T, Jyske T, Peltoniemi M, Sterck F, von Arx G, et al. Osmolality and non-structural carbohydrate composition in the secondary phloem of trees across a latitudinal gradient in Europe. Front Plant Sci. 2016;7:726.
31. Velikova V, Loreto F. On the relationship between isoprene emission and thermotolerance in *Phragmites australis* leaves exposed to high temperatures and during the recovery from a heat stress. Plant Cell Environ. 2005;28:318–27.
32. Chaparzadeh N, D'Amico ML, Khavari-Nejad RA, Izzo R, Navari-Izzo F. Antioxidative responses of *Calendula officinalis* under salinity conditions. Plant Physiol Biochem. 2004;42(9):695–701.
33. Cheeseman JM. Hydrogen peroxide concentrations in leaves under natural conditions. J Exp Bot. 2006;57(10):2435–44.

34. Ferreira RB, Monteiro S, Freitas R, Santos CN, Chen Z, Batista LM, et al. The role of plant defence proteins in fungal pathogenesis. Mol Plant Pathol. 2007;8(5):677–700.
35. Pusztahelyi T. Chitin and chitin-related compounds in plant-fungal interactions. Mycology. 2018;9(3):189–201.
36. Bari R, Jones JD. Role of plant hormones in plant defence responses. Plant Mol Biol. 2009;69(4):473–88.
37. Shigenaga AM, Argueso CT. No hormone to rule them all: interactions of plant hormones during the responses of plants to pathogens. Semin Cell Dev Biol. 2016;56:174–89.
38. Steenackers W, El Houari I, Baekelandt A, Witvrouw K, Dhondt S, Leroux O, et al. *cis*-Cinnamic acid is a natural plant growth-promoting compound. J Exp Bot. 2019;70(21):6293–304.
39. McAdam SA, Brodribb TJ, Ross JJ. Shoot-derived abscisic acid promotes root growth. Plant Cell Environ. 2016;39(3):652–9.
40. De Smet I, Signora L, Beeckman T, Inze D, Foyer CH, Zhang H. An abscisic acid-sensitive checkpoint in lateral root development of *Arabidopsis*. Plant J. 2003;33:543–55.
41. De Smet I, Zhang H, Inze D, Beeckman T. A novel role for abscisic acid emerges from underground. Trends Plant Sci. 2006;11(9):434–9.
42. Li X, Chen L, Forde BG, Davies WJ. The biphasic root growth response to abscisic acid in Arabidopsis involves interaction with ethylene and auxin signalling pathways. Front Plant Sci. 2017;8:1493.
43. Harris JM. Abscisic acid: hidden architect of root system structure. Plants (Basel). 2015;4(3):548–72.
44. Obianom C, Romanazzi G, Sivakumar D. Effects of chitosan treatment on avocado postharvest diseases and expression of phenylalanine ammonia-lyase, chitinase and lipoxygenase genes. Postharvest Biol Technol. 2019;147:214–21.
45. Coqueiro DS, de Souza AA, Takita MA, Rodrigues CM, Kishi LT, Machado MA. Transcriptional profile of sweet orange in response to chitosan and salicylic acid. BMC Genom. 2015;16:288.
46. van Bakel H, Stout JM, Cote AG, Tallon CM, Sharpe AG, Hughes TR, et al. The draft genome and transcriptome of *Cannabis sativa*. Genome Biol. 2011;12:R102.
47. Ye J, Coulouris G, Zaretskaya I, Cutcutache I, Rozen S, Madden TL. Primer-BLAST: A tool to design target-specific primers for polymerase chain reaction. BMC Bioinformatics. 2012;13:134.
48. Hadwiger LA, Tanaka K. DNA damage and chromatin conformation changes confer nonhost resistance: a hypothesis based on effects of anti-cancer agents on plant defense responses. Front Plant Sci. 2018;9:1056.
49. Sathya U, Nithya M, Keerthi. Fabrication and characterisation of fine-tuned Polyetherimide (PEI)/WO3 composite ultrafiltration membranes for antifouling studies. Chem Phys Lett. 2020;744:137201.
50. Kumar A, Yap WT, Foo SL, Lee TK. Effects of sterilization cycles on PEEK for medical device application. Bioengineering (Basel). 2018;5:18.
51. Tee YL, Peng C, Pille P, Leary M, Tran P. PolyJet 3D printing of composite materials: experimental and modelling approach. JOM. 2020;72(3):1105–17.

52. Pichyangkura R, Chadchawan S. Biostimulant activity of chitosan in horticulture. Sci Hortic. 2015;196:49–65.
53. Kim H-J, Chen F, Wang X, Rajapakse NC. Effect of chitosan on the biological properties of sweet basil (*Ocimum basilicum* L.). J Agric Food Chem. 2005;53:3696–701.
54. de Jail NG, Luiz C, da Rocha Neto AC, Di Piero RM. High-density chitosan reduces the severity of bacterial spot and activates the defense mechanisms of tomato plants. Trop Plant Pathol. 2014;39(6):434–41.
55. Chien P-J, Sheu F, Yang F-H. Effects of edible chitosan coating on quality and shelf life of sliced mango fruit. J Food Eng. 2007;78(1):225–9.
56. Hadwiger LA. Multiple effects of chitosan on plant systems: solid science or hype. Plant Sci. 2013;208:42–9.
57. Gong BQ, Wang FZ, Li JF. Hide-and-seek: chitin-triggered plant immunity and fungal counterstrategies. Trends Plant Sci. 2020;25(8):805–16.
58. Yin H, Du Y, Dong Z. Chitin oligosaccharide and chitosan oligosaccharide: two similar but different plant elicitors. Front Plant Sci. 2016;7:522.
59. Lopez-Moya F, Suarez-Fernandez M, Lopez-Llorca LV. Molecular mechanisms of chitosan interactions with fungi and plants. Int J Mol Sci. 2019;20(2).
60. Malerba M, Cerana R. Chitosan effects on plant systems. Int J Mol Sci. 2016;17(7).
61. Suarez-Fernandez M, Marhuenda-Egea FC, Lopez-Moya F, Arnao MB, Cabrera-Escribano F, Nueda MJ, et al. Chitosan induces plant hormones and defenses in tomato root exudates. Front Plant Sci. 2020;11:572087.
62. Berens ML, Berry HM, Mine A, Argueso CT, Tsuda K. Evolution of hormone signaling networks in plant defense. Annu Rev Phytopathol. 2017;55:401–25.
63. Sharp R. A review of the applications of chitin and its derivatives in agriculture to modify plant-microbial interactions and improve crop yields. Agronomy. 2013;3(4):757–93.
64. Olicon-Hernandez DR, Vazquez-Landaverde PA, Cruz-Camarillo R, Rojas-Avelizapa LI. Comparison of chito-oligosaccharide production from three different colloidal chitosans using the endochitonsanolytic system of *Bacillus thuringiensis*. Prep Biochem Biotechnol. 2017;47(2):116–22.
65. Shen CR, Chen YS, Yang CJ, Chen JK, Liu CL. Colloid chitin azure is a dispersible, low-cost substrate for chitinase measurements in a sensitive, fast, reproducible assay. J Biomol Screen. 2010;15(2):213–7.
66. Cao D, Lutz A, Hill CB, Callahan DL, Roessner U. A quantitative profiling method of phytohormones and other metabolites applied to barley roots subjected to salinity stress. Front Plant Sci. 2016;7:2070.
67. Chong J, Soufan O, Li C, Caraus I, Li S, Bourque G, et al. MetaboAnalyst 4.0: towards more transparent and integrative metabolomics analysis. Nucleic Acids Res. 2018;46(W1):W486-W94.

Figures

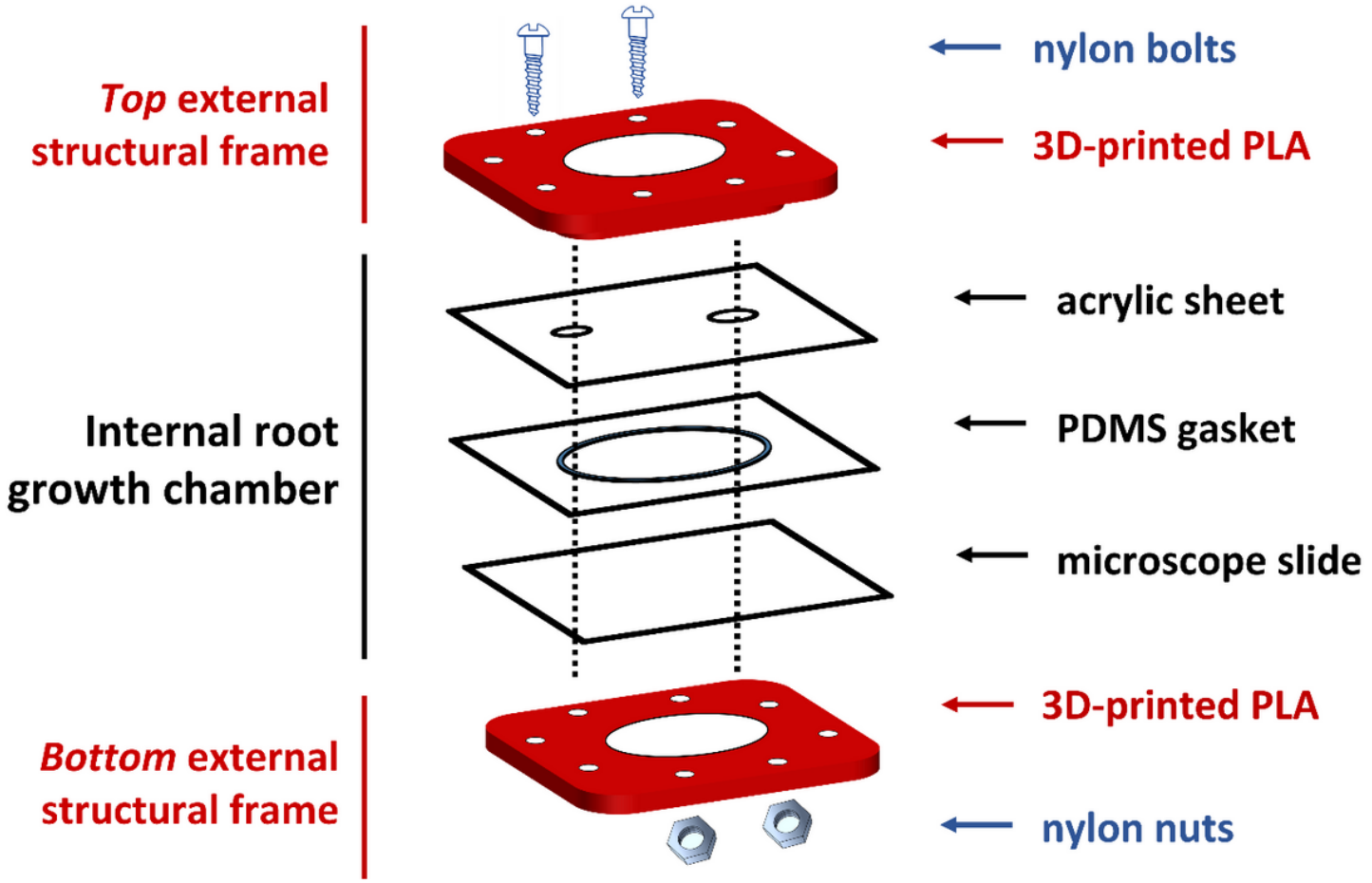

Figure 1

Exploded-view diagram displaying the main components of Root-TRAPR system. The internal root growth chamber is composed of an upper acrylic sheet, a customized PDMS gasket and a bottom microscope slide. The external structural frames (top and bottom) are made of 3D-printed PLA plastic, which is retained with nylon bolts and nuts (×8). All components are stable to ethanol, facilitating decontamination and sterilization.

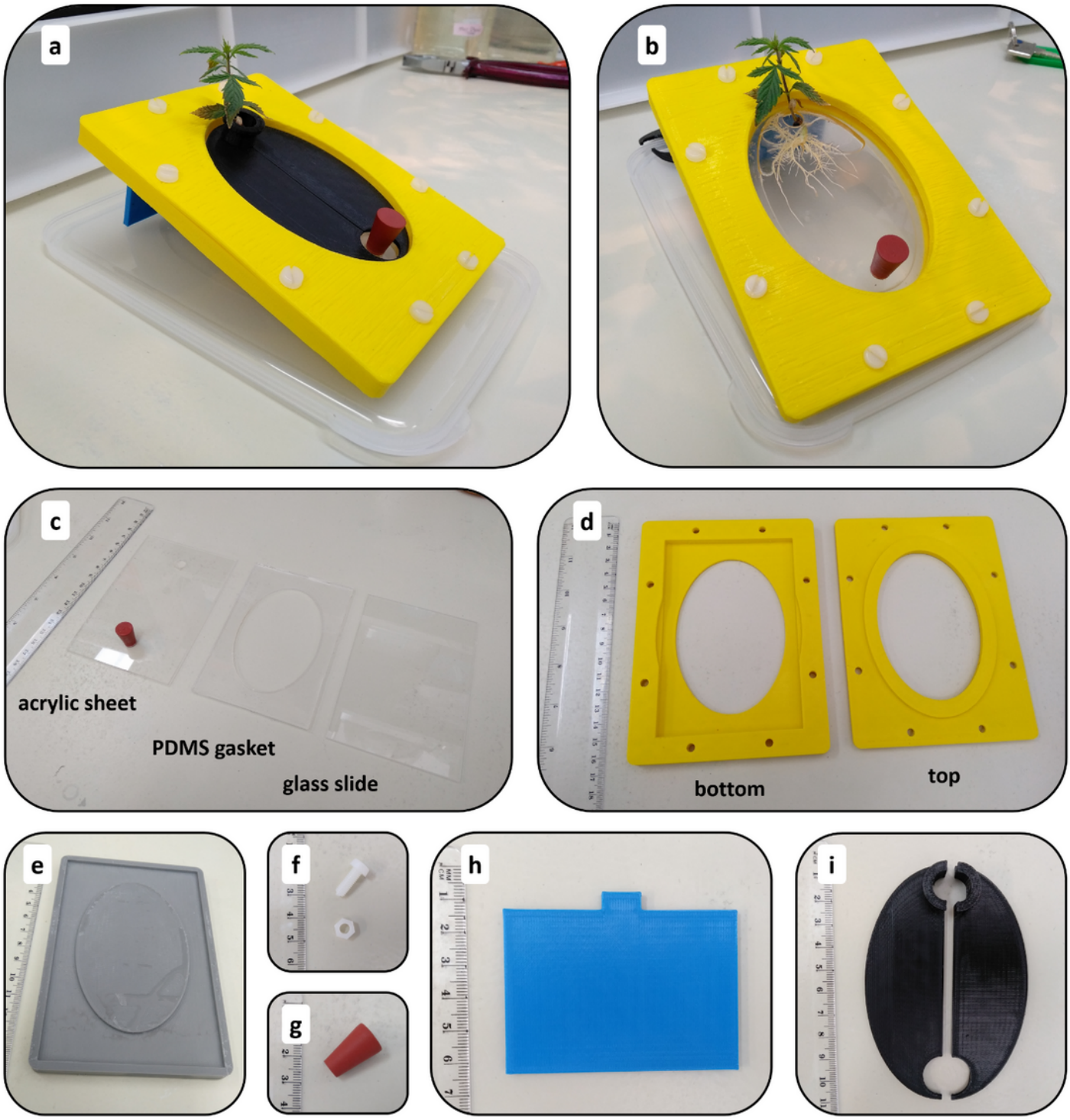

Figure 2

Pictures displaying a complete assembled Root-TRAPR system with industrial hemp grown inside (a and b) and all individual parts (c-i) – the internal root growth chamber consisting of an acrylic sheet, a PDMS gasket and a microscope slide (c), top and bottom external structural frames (d), PDMS mold (e), nylon bolts and nuts (f), rubber bung (g), stand (h) and window shutter (i).

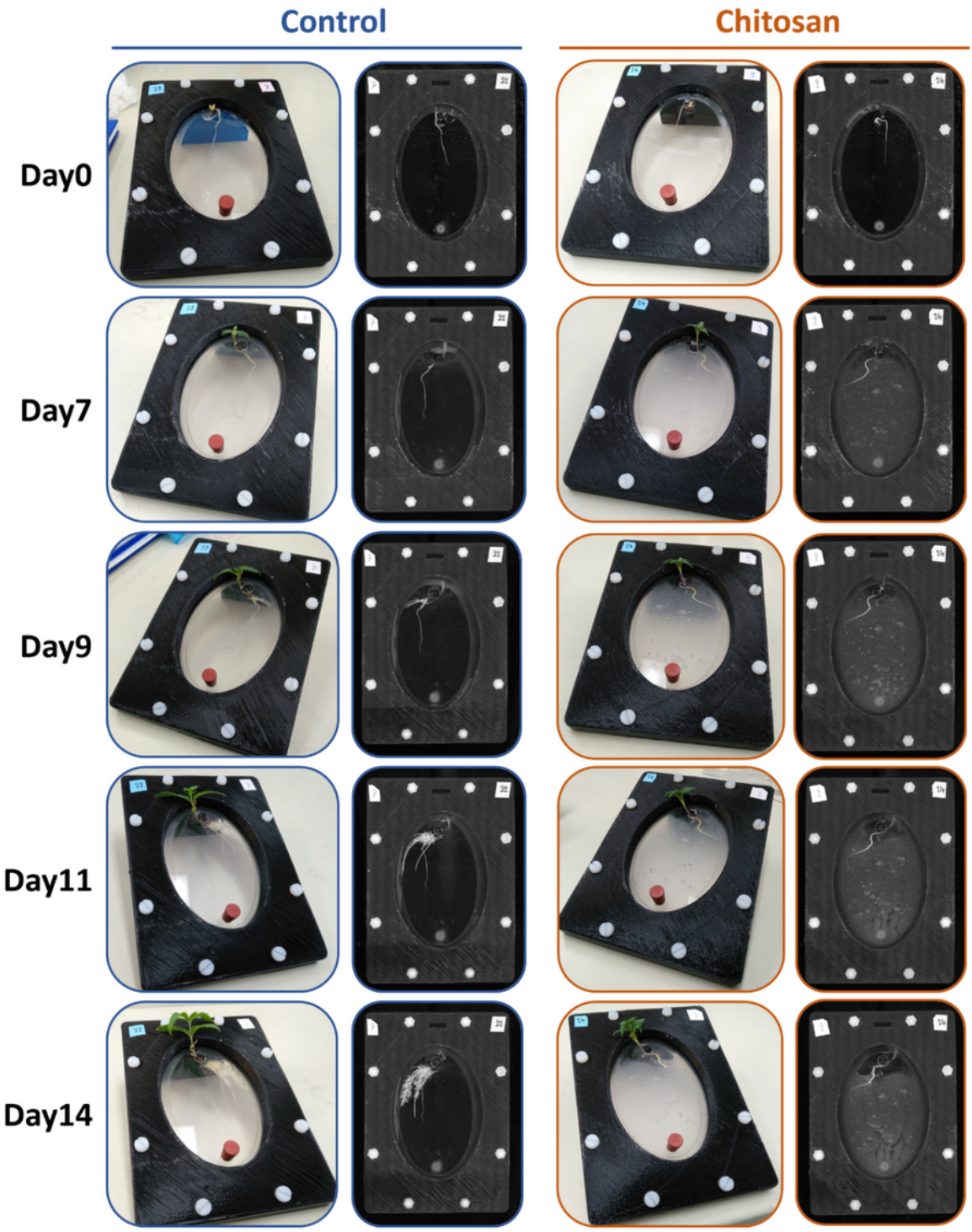

Figure 3

Representative photographs presenting sequential development of industrial hemp in Root-TRAPR system comparing between control and chitosan-treated condition from day 0 to day 14. Chitosan treatment was conducted on day 7 of the experiment. The top-view photos were taken on a smartphone camera and root structures were captured using a WinRHIZO root scanner.

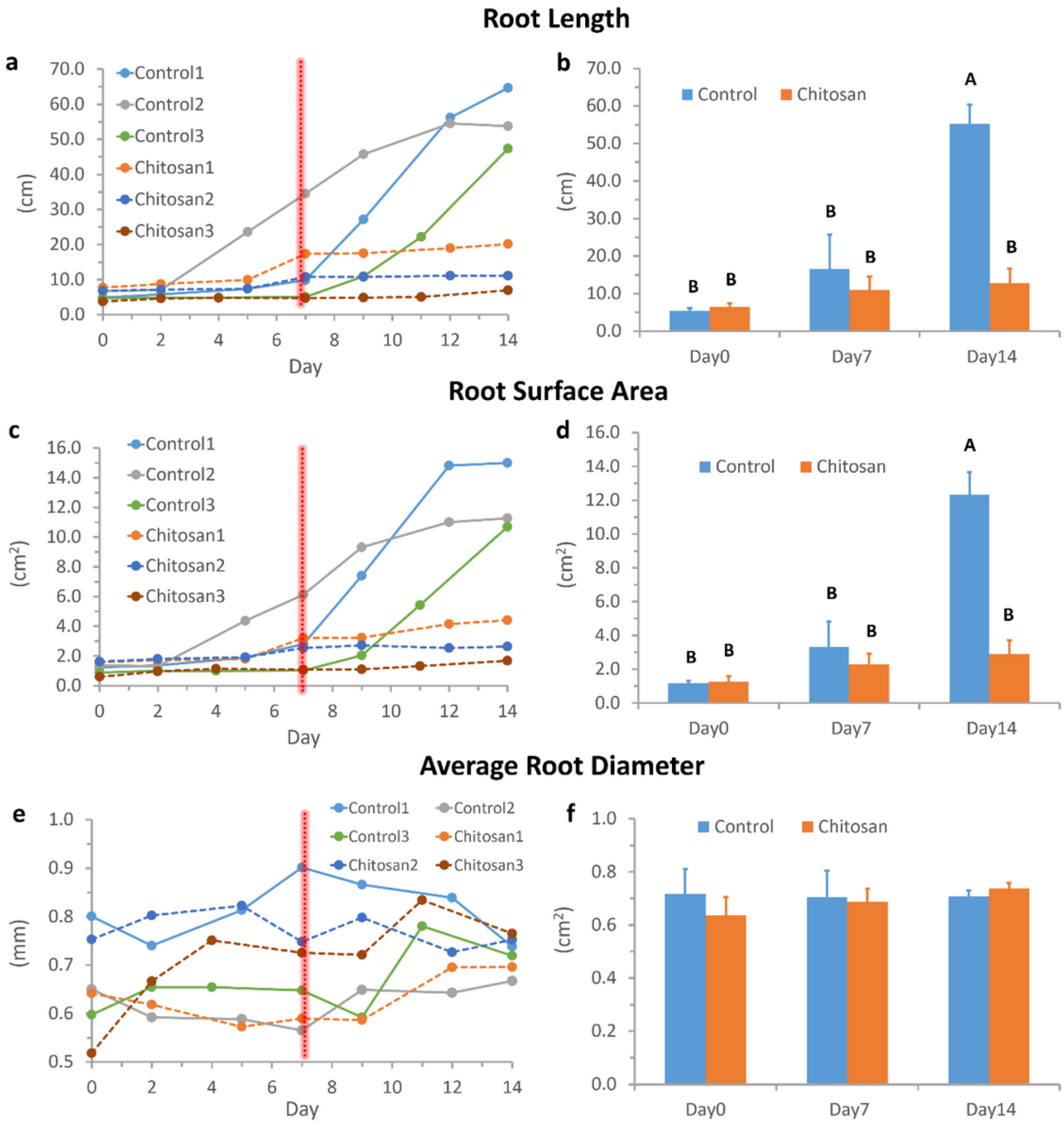

Figure 4

Graphs depicting root developments of industrial hemp in Root-TRAPR system comparing between control and chitosan-treated plants. The measurements are root length (a and b), root surface area (c and d), and average root diameter (e and f). Line graphs (a, c and e) display root development of three individual replicates of each group. Bar graphs (b, d and f) show an average with an error bar of standard error of the mean (SEM). Different capital letters above bar graph (A and B) refer to a significant

difference at p-value < 0.05 tested by one-way ANOVA, followed by Tukey's HSD test across treatment and day.

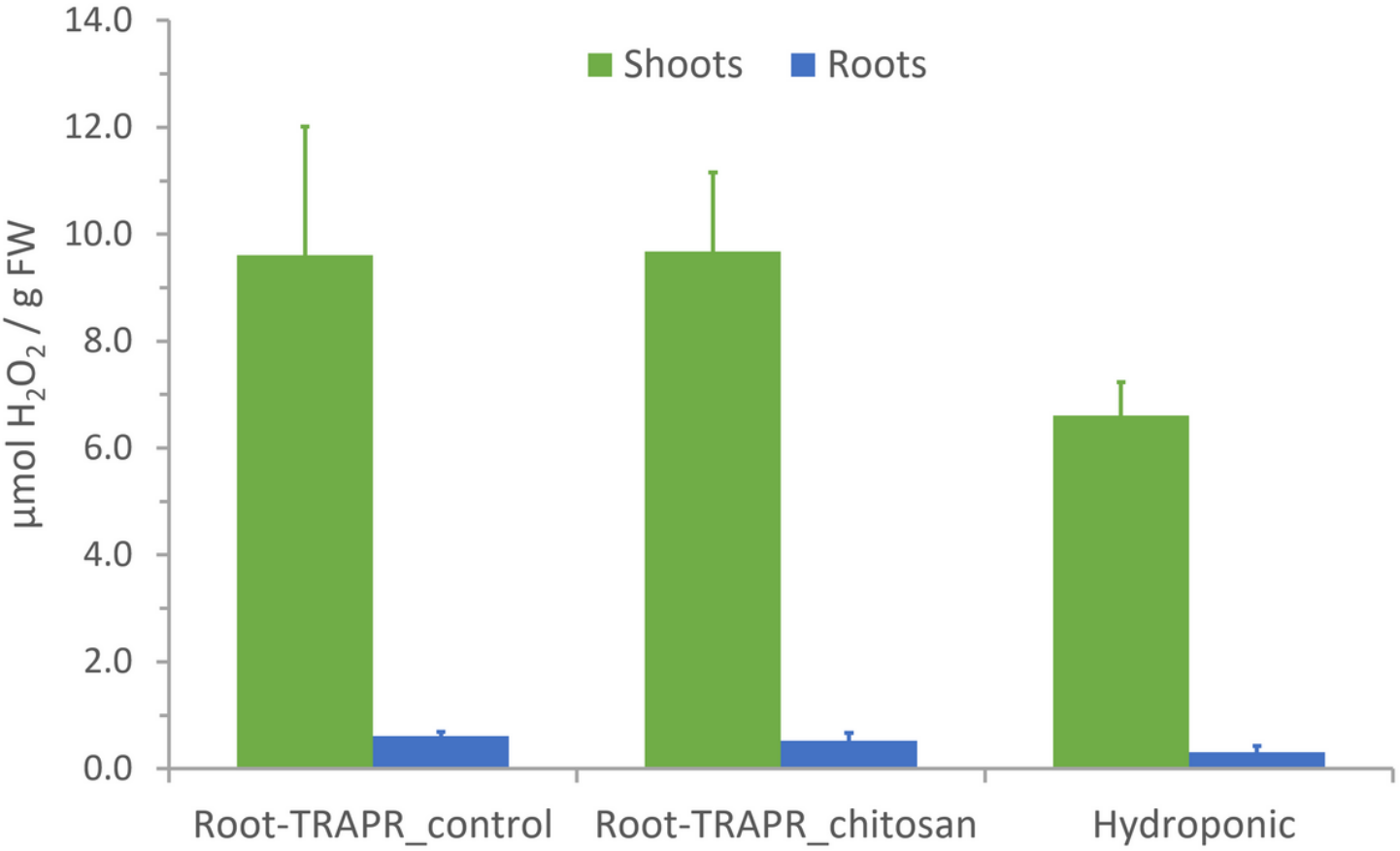

Figure 5

Hydrogen peroxide contents measured from shoots and roots of control and chitosan-treated plants grown in Root-TRAPR systems in comparison with the plants grown in normal hydroponic solution. Values are an average of three biological replicates displaying SEM in error bar. Statistical one-way ANOVA with Tukey's HSD test was used to compare the means across three conditions within the same tissue types, but statistically significant differences were not observed.

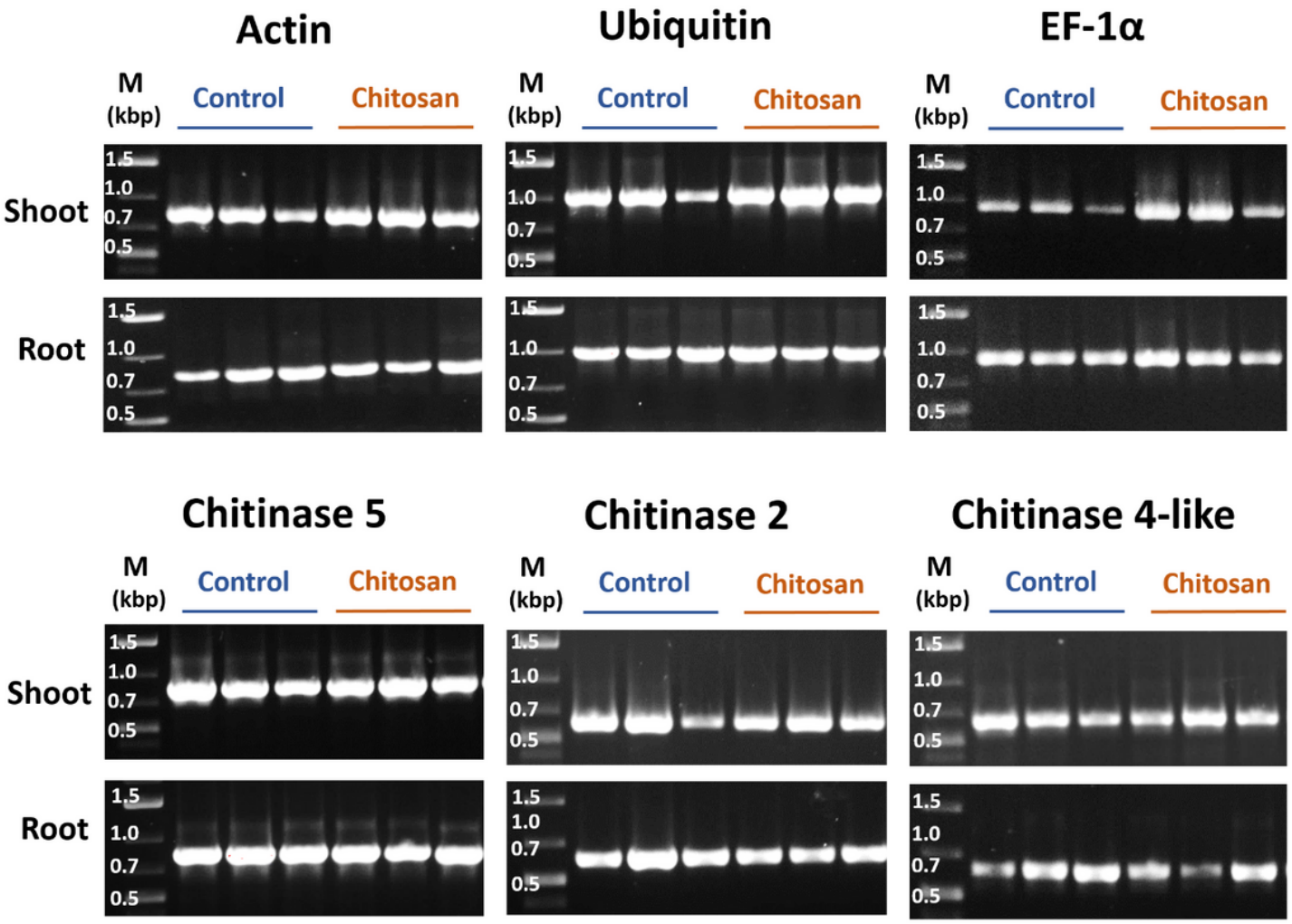

Figure 6

Gel images showing endpoint PCR products of 6 C. sativa genes including actin, ubiquitin, EF-1α, chitinase 5, chitinase 2 and chitinase 4-like comparing between three biological replicates of control and chitosan-treated plants in both shoot and root tissues. M is a DNA marker (GeneRuler 1 kb plus, Thermo Scientific) with DNA sizes in kilo base pair (kbp) unit.

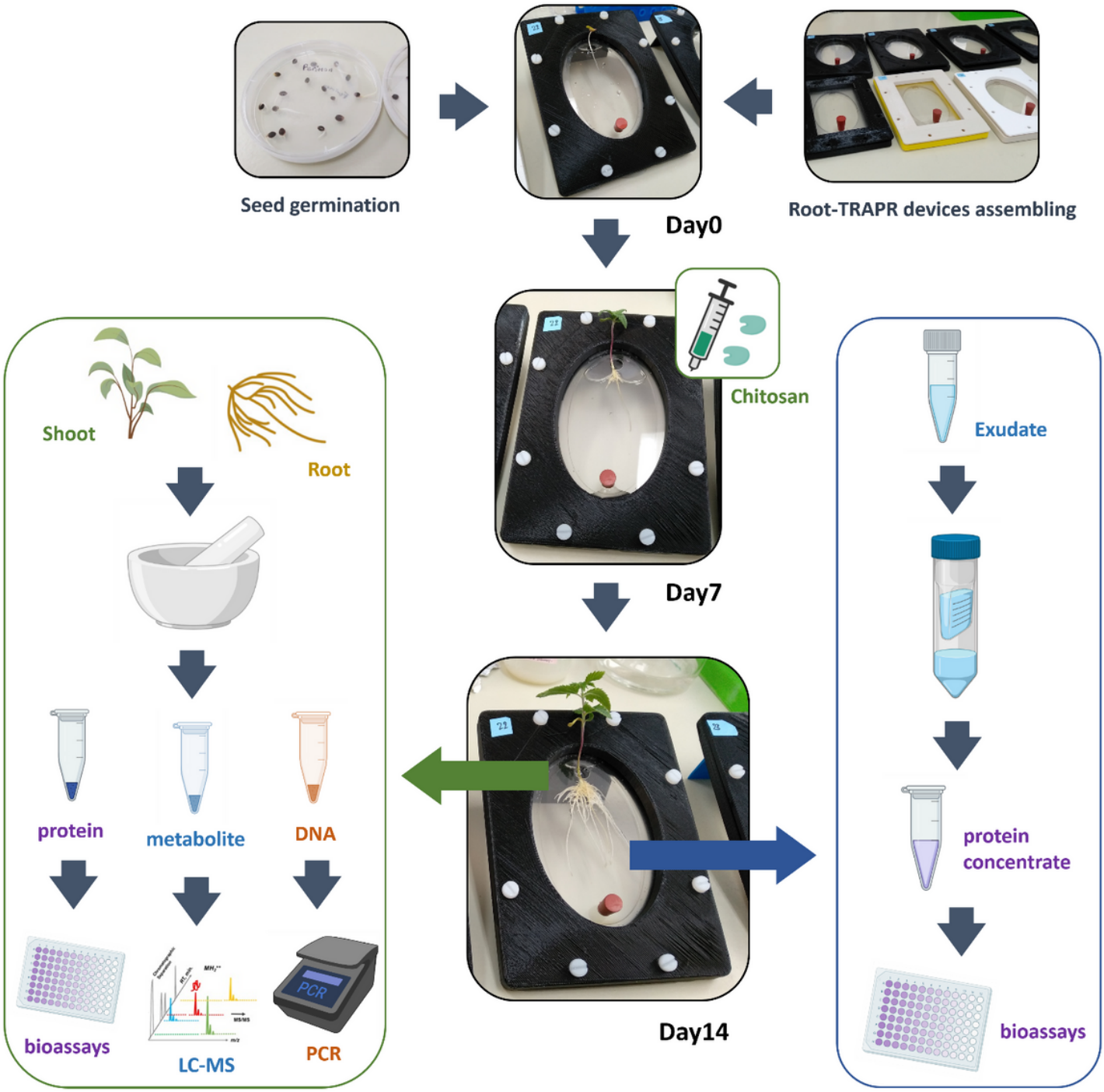

Figure 7

Summarized workflow of plant growth experiment in this study. First, industrial hemp seeds were germinated in petri dishes, while Root-TRAPR systems were assembled. Seedlings were transferred to Root-TRAPR systems on day 0. Chitosan treatment was performed on day 7. Plant tissues (shoot and root) and root exudate were sampled on day 14. Tissue samples were ground and divided into three parts for subsequent analyses. They were analyzed for bioassays (protein), phytohormone quantification (metabolite) and gene detection (DNA). Root exudate was passed through a 10 kDa MWCO Amicon

centrifugal filter device (Merck Millipore, Germany) to concentrate proteins, which were then tested for enzyme activities. This figure was partially created with BioRender.com.

Supplementary Files

This is a list of supplementary files associated with this preprint. Click to download.

- 20210727AdditionalFile1.docx
- 20210727AdditionalFile2.png
- 20210727AdditionalFile3.png
- 20210727AdditionalFile4.png
- 20210727AdditionalFile5.xlsx
- 20210727AdditionalFile6.stl
- 20210727AdditionalFile7.stl
- 20210727AdditionalFile8.stl
- 20210727AdditionalFile9.stl
- 20210727AdditionalFile10.stl
- 20210727AdditionalFile11.stl